Random Changes of Flow Topology in Two-Dimensional and Geophysical Turbulence

Freddy Bouchet* and Eric Simonnet
INLN, CNRS, UNSA, 1361 route des lucioles, 06560 Valbonne, France
(Received 17 April 2008; published 4 March 2009)

We study the two-dimensional (2D) stochastic Navier-Stokes (SNS) equations in the inertial limit of weak forcing and dissipation. The stationary measure is concentrated close to steady solutions of the 2D Euler equations. For such inertial flows, we prove that bifurcations in the flow topology occur either by changing the domain shape, the nonlinearity of the vorticity–stream-function relation, or the energy. Associated with this, we observe bistable behavior in SNS with random changes from dipoles to unidirectional flows. The theoretical explanation being very general, we infer the existence of similar phenomena in experiments and in some regimes of geophysical flows.

DOI: 10.1103/PhysRevLett.102.094504 PACS numbers: 47.27.−i, 05.40.Ca, 47.27.E−, 92.60.hk

The largest scales of turbulent flows are at the heart of a number of geophysical processes: climate, meteorology, ocean dynamics, Earth's magnetic field. Earth is affected on a very large range of time scales, up to millennia, by the structure and variability of these flows. Many of these undergo extreme and abrupt qualitative changes, seemingly randomly, after very long periods of apparent stability. This occurs for instance for magnetic field reversal for the Earth or in MHD experiments [1], for 3D flows [2], for multiple equilibria of atmospheric flows [3], for 2D turbulence experiments [4,5], and for the paths of the Kuroshio current [6].

Understanding these phenomena requires a statistical description of the largest scales of turbulent flows. Very few theoretical approaches exist due to the prohibitively huge number of degrees of freedom involved. In the following, we argue that 2D turbulence, because of its relative theoretical simplicity, is a very interesting framework to understand these phenomena. We predict the existence of random switches from dipoles to unidirectional flows (see Fig. 1), in the 2D Navier-Stokes equations with random force (SNS). We first exhibit bifurcation lines representing abrupt changes in steady solutions in the inertial limit and then look for the corresponding transitions in numerical simulations. Applications to geophysical and experimental flows is discussed in the conclusion.

Geophysical and 2D inviscid flows are characterized by energy and enstrophy conservation and an infinite number of (Casimir) invariants. This property prevents direct energy cascade towards the small scales, by contrast with 3D turbulence. The first consequence is an inverse energy cascade towards the large scales and a direct enstrophy cascade. Kraichnan classical theory [7] studies the self-similar processes associated with these two cascades. The second phenomenon, the self-organization of the flow into jets and vortices, occurs if energy is not dissipated before reaching the largest scale. Then coherent structures break the self-similarity so that their study cannot be properly addressed using Kraichnan theory [7]. A second classical theory, the so-called Robert-Sommeria-Miller (RSM) equilibrium statistical mechanics [8], predicts the self-organized structures for inviscid decaying turbulence. However, this inviscid theory does not take into account the long-term effects of forcing and dissipation as well as the slow dynamics of the flow. Therefore, random changes of flow topologies cannot be explained by these two classical theories.

As an alternative theoretical approach, we study statistically stationary states of SNS equation. Note that a self-similar growth of a dipole has been studied in [9] emphasizing transient growths: both approaches complement each other. SNS equation on a doubly periodic domain $\mathcal{D} = (0; 2\pi\delta) \times (0; 2\pi)$ reads

$$\frac{\partial \omega}{\partial t} + \mathbf{v}\cdot\boldsymbol{\nabla}\omega = -\alpha\omega + \nu\Delta\omega + \sqrt{\sigma}\eta, \qquad \mathbf{v} = \mathbf{e}_z \times \boldsymbol{\nabla}\psi, \qquad \omega = \Delta\psi, \tag{1}$$

where ω, $\mathbf{v}$, and ψ are, respectively, the vorticity, velocity, and stream function; α is the Rayleigh friction coefficient and ν the viscosity. The curl of the forcing is $\eta = \sum_{\mathbf{k}} f_{\mathbf{k}}\eta_{\mathbf{k}}(t)e^{i\mathbf{k}\cdot\mathbf{x}}/(2\pi)$, with $\{\eta_{\mathbf{k}}\}$ independent Gaussian white noises: $\langle \eta_{\mathbf{k}}(t)\eta_{\mathbf{k}'}(t')\rangle = \delta_{\mathbf{k}\mathbf{k}'}\delta(t-t')$. We impose $B_0 \equiv \sum_{\mathbf{k}}|f_{\mathbf{k}}|^2/|\mathbf{k}|^2 = 1$ so that σ is the average energy injection rate.

Euler equations ($\alpha = \nu = \sigma = 0$) conserve the kinetic energy E and vorticity moments Ω_n (Ω_2 is the enstrophy)

$$E = \frac{1}{2}\int_{\mathcal{D}} d^2x\mathbf{v}^2 \quad \text{and} \quad \Omega_n = \int_{\mathcal{D}} d^2x\omega^n. \tag{2}$$

Application of Ito formula to the energy, and averaging over the noise, leads to $d\langle E\rangle/dt = -2\alpha\langle E\rangle + \sigma - \nu\langle\Omega_2\rangle$. If $\langle . \rangle_S$ denotes averages over the stationary measure, we have $2\alpha\langle E\rangle_S + \nu\langle\Omega_2\rangle_S = \sigma$. It expresses the balance between energy injection and energy dissipation. Clearly, for flows with energetic large scales, Rayleigh friction dominates dissipation $2\alpha\langle E\rangle_S \gg \nu\langle\Omega_2\rangle_S$ (we consider the limit $\nu \to 0$ for fixed α and assume $\nu\langle\Omega_2\rangle_S \to 0$). Dimensionless equation with time change $t' = \sqrt{\sigma/(2\alpha)}t$, $\omega' = \sqrt{2\alpha/\sigma}\omega$, $\alpha' = (2\alpha)^{3/2}/(2\sigma^{1/2})$, and $\nu' = \nu(2\alpha/\sigma)^{1/2}$ are

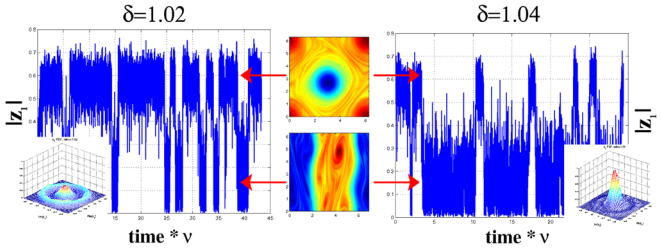

FIG. 1 (color online). Time series and probability density functions (PDFs) for the order parameter z_1 (see page 3) illustrating random changes between dipoles and unidirectional flows. Colored insets: vorticity fields.

$$\frac{\partial \omega}{\partial t} + \mathbf{v}\cdot\boldsymbol{\nabla}\omega = -\alpha\omega + \nu\Delta\omega + \sqrt{2\alpha}\eta. \tag{3}$$

The energy balance now reads $\langle E\rangle_S + (\nu/2\alpha)\langle\Omega_2\rangle_S = 1$. For many geophysical flows and experiments, the case of weak forces and dissipation is the relevant one. We thus study the inertial limit $\alpha \ll 1$ ($\lim_{\alpha\to 0}\lim_{\nu\to 0}$).

Without Rayleigh friction ($\alpha = 0$), the balance relation becomes $2\nu\langle\Omega_2\rangle_S = \sigma$. By a time unit change, we can fix $\langle\Omega_2\rangle_S = 1$. The nondimensional equation is then

$$\frac{\partial \omega}{\partial t} + \mathbf{v}\cdot\boldsymbol{\nabla}\omega = \nu\Delta\omega + \sqrt{2\nu}\eta. \tag{4}$$

Equation (4) is less physically relevant than (3) but is still very interesting from an academic point of view. A series of works has proved very interesting mathematical results, including properties of stationary measures in the inertial limit $\nu \to 0$ (see [10] and references therein). All the following considerations are relevant for both models (3) and (4), in their respective inertial limits.

We know since decades from real [11] or numerical experiments [5,12] that for times large compared to the turnover time but small compared to the dissipation time, the largest scales of 2D Navier-Stokes turbulent flows converge towards steady solutions of Euler equations:

$$\mathbf{v}\cdot\boldsymbol{\nabla}\omega = 0 \quad \text{or equivalently} \quad \omega = f(\psi). \tag{5}$$

It appears to be true as well for the Euler equations. For instance, RSM theory predicts f from given initial conditions. Given this empirical evidence, it is thus extremely natural to expect that in the inertial limit, SNS measures are concentrated near steady Euler flows.

The ensemble of steady Euler flows is huge, being parametrized by the function f. It will be proven that when either f or the domain shape is changed, bifurcations can occur. Such abrupt transitions lead to strong qualitative changes in the flow topology. In this critical regime and under the action of a small random force in the SNS equation, the system switches randomly from one type of topology to another. In the following, we show numerical evidence that this scenario is valid.

We study a bifurcation diagram for stable steady Euler solutions, by considering

$$S(E) = \sup_{\omega}\left\{\mathcal{S}[\omega] = \int_{\mathcal{D}} d^2x s(\omega) | \mathcal{E}(\omega) = E\right\}, \tag{6}$$

where $S(E)$ is the equilibrium "entropy," $\mathcal{S}$ the "entropy" of ω. The specific "entropy" s is concave. We assume s even, and with a local maxima for $\omega = 0$, for simplicity. At this stage, s is arbitrary, but we show in the following that, in the limit of low energy, the detailed shape for s is unimportant except for the coefficient a_4 defined by $s(\omega) = -\omega^2/2 + a_4\omega^4/4 + \mathcal{O}(\omega^4)$. Critical points of (6) verify $\omega = f(\psi) = (s')^{-1}(-\beta\psi)$, where β is the Lagrange multiplier associated with energy conservation. They are thus steady Euler flows, satisfying (5), and the knowledge of f or s are equivalent. The Lyapounov stability of maxima of (6) can be proven using Arnold theorems [13(a),13(b)] or their generalizations. One can also prove that any solutions for (6) are RSM equilibria [14]. Even if it seems appealing, there are no clear theoretical arguments for giving a thermodynamical interpretation to (6) in the SNS out-of-equilibrium context, and the term entropy is used here by analogy only. We thus consider (6) only as a practical way to describe *stable* steady Euler solutions.

Dipoles and unidirectional flows ("bars") have been obtained numerically [15] as entropy maxima for the 2D Euler equations, in a doubly periodic domain, assuming sinh, tanh, and 3-level Poisson $\omega - \psi$ (5) relations. According to [15], "Which has the greater entropy (between dipoles and bars) depends on seemingly arbitrary choices." We explain in the following that a_4 and E are the important control parameters.

The fact that both unidirectional flows and dipole may be equilibria can be understood from the small energy limit of (6). Let us call $\{e_i\}_{i\geq 1}$ the orthonormal family of eigenfunctions of the Laplacian $-\Delta e_i = \lambda_i e_i, \langle e_i e_j\rangle_{\mathcal{D}} = \delta_{ij}$ ($\langle . \rangle_{\mathcal{D}} \equiv \int_{\mathcal{D}} dx$ and λ_i are arranged in increasing order). We decompose the vorticity as $\omega = \sum_{i\geq 1}\omega_i e_i$. The energy is then $2\mathcal{E}(\omega) = \sum_{i\geq 1}\lambda_i^{-1}\omega_i^2$. Since $\mathcal{E}(\omega)$ is always positive, $\langle\omega^2\rangle_{\mathcal{D}}$ is small in the limit $E \to 0$, and only the quadratic part of s is relevant. Then computation of (6) is straightforward and gives

$$\omega \sim_{E\to 0} (2\lambda_1 E)^{1/2} e_1 \quad \text{with } S(E) = -\lambda_1 E + \mathcal{O}(a_4\lambda_1^2 E^2). \tag{7}$$

We thus conclude that the eigenmode with the smallest eigenvalue, e_1, is selected, corresponding to the heuristic idea that energy condensates to the largest scale. For instance, when the aspect ratio $\delta > 1$, the mode $e_1 = n_1 \sin[(x+\phi_1)/\delta]$, $\lambda_1 = 1/\delta^2$ is selected. It is an unidirectional velocity field $\mathbf{v}_1 = n_1\cos[(x+\phi_1)/\delta]\mathbf{e}_y$ where ϕ_1 is a phase associated to the translational invariance. A dipole is actually a mixed state $\alpha e_1 + \beta e_2$ with $e_2 = n_2\sin(y+\phi_2)$, $\lambda_2 = 1$. In the weak energy limit, it can thus be selected only in the situation $\lambda_1 \simeq \lambda_2$, which happens for the square box $\delta = 1$. On the one hand, for $\lambda_1 = \lambda_2$, we prove bellow that higher-order terms in (7), of order $a_4\lambda_1^2 E^2$, select between dipoles and unidirectional flows. We note that a_4 is intimately related to the shape of the

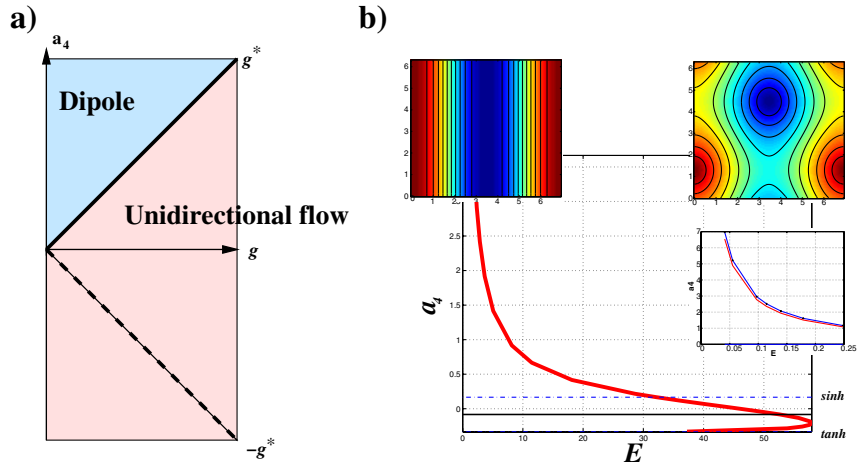

FIG. 2 (color online). Bifurcation diagrams for steady Euler flows. (a) In the g-a_4 plane (g is the relative effect of geometry and energy $g = (1/\delta^2 - 1)/E$ and a_4 is the $\omega - \psi$ nonlinearity); (b) For a doubly-periodic geometry with aspect ratio $\delta = 1.1$ in the $a_4 - E$ plane and from numerical computations. The hyperbola curve is the bifurcation line between unidirectional flows and dipoles (colored insets are stream-function patterns). The small inset compares numerical and theoretical bifurcation lines for $\delta = 1.01$.

relationship $\omega = f(\psi) = (s')^{-1}(-\beta\psi)$. Indeed, $(s')^{-1} \times (-x) = x + a_4 x^3 + o(x^3)$ and when $a_4 > 0$ (resp. $a_4 < 0$), the curve $f(\psi)$ bends upward (resp. downward) for positive ψ similarly to sinh (resp. tanh). On the other hand, the entropy difference between states e_1 and e_2 is equivalent to $(\lambda_2 - \lambda_1)E$ ($\lambda_{1,2}$ depend only on the domain shape). We thus conclude that the domain shape selects the equilibria for $\lambda_2 - \lambda_1 \gg a_4\lambda_1^2 E$ whereas for $\lambda_2 - \lambda_1 \ll a_4\lambda_1^2 E$, the degeneracy between pure (unidirectional) and mixed (dipole) states is removed by the nonlinearity of f (i.e., a_4).

In order to study more precisely the parameter range where the bifurcation occurs, we define g by $\lambda_2 - \lambda_1 = gE$. In the small energy limit $E \to 0$, for fixed g, long but straightforward computations of (6) lead to

$$S(E) \sim_{E\to 0} -\lambda_1 E + E^2 \max_{0\le X\le 1} h(X), \tag{8}$$

with $h(X) = \langle e_1^4\rangle_{\mathcal{D}} a_4 \lambda_1^2 - gX + 2\gamma\lambda_1^2 a_4 X(1-X)$, where $\gamma = 3\langle e_1^2 e_2^2\rangle_{\mathcal{D}} - \langle e_1^4\rangle_{\mathcal{D}} > 0$. The vorticity equilibria are then $\omega_{\text{eq}} \sim_{E\to 0} \sqrt{2\lambda_1 E(1-X_M)}e_1 + \sqrt{2E\lambda_1 X_M}e_2$ where X_M is the maximizer of h in (8). For $X_M = 0$ or $X_M = 1$, ω_{eq} is an unidirectional flow whereas for $0 < X_M < 1$, it is a dipole (symmetric for $X_M = 1/2$). The selection occurs via maximization of h.

The resulting bifurcation diagram is summarized in Fig. 2(a). When maximizing h, the sign of a_4 plays a crucial role. When $g = 0$, the dipole is selected for $a_4 > 0$ (sinh-like), whereas unidirectional flows are selected for $a_4 < 0$ (tanh-like). The term $-gX$, in h, favors the pure state e_1 ($X = 0$). For $a_4 < 0$, the unidirectional flow e_1 is always selected. Interestingly, for $a_4 > 0$ a bifurcation occurs along the critical line $g^\star = 2\gamma\lambda_1^2 a_4$ between dipole and unidirectional flows.

For theoretical reasons, we had to use g; however, for the geometry of interest here, the aspect ratio δ is the relevant physical parameter. Using the relation $g = (\lambda_2 - \lambda_1)/E$, we obtain that the critical line in the $E - a_4$ plane [Fig. 2(b)] is the hyperbola $a_4 E = 8\pi^2(\delta - 1)/3 + o(\delta - 1)$. We use a continuation algorithm in order to numerically compute solutions to (6) with $f_{a_4}(x) = (1/3 - 2a_4) \times \tanh x + (2/3 + 2a_4)\sinh x$. The inset in Fig. 2(b) shows good agreement for transition lines obtained either numerically or theoretically at low energy and for $\delta = 1.01$. The bifurcation diagram for $\delta = 1.1$ is given as well. In this case, the transition line is qualitatively similar (close to a hyperbola), even if the coefficient defining the hyperbola is no more correctly determined using the low-energy limit.

We expect to observe both dipoles and unidirectional flows in SNS. Numerical simulations in a square domain $\delta = 1$ exhibit statistically stationary ω with a dipole structure [Fig. 3(a)], whereas for $\delta \ge 1.1$, nearly unidirectional flows are observed [Fig. 3(b)]. This result has been con-

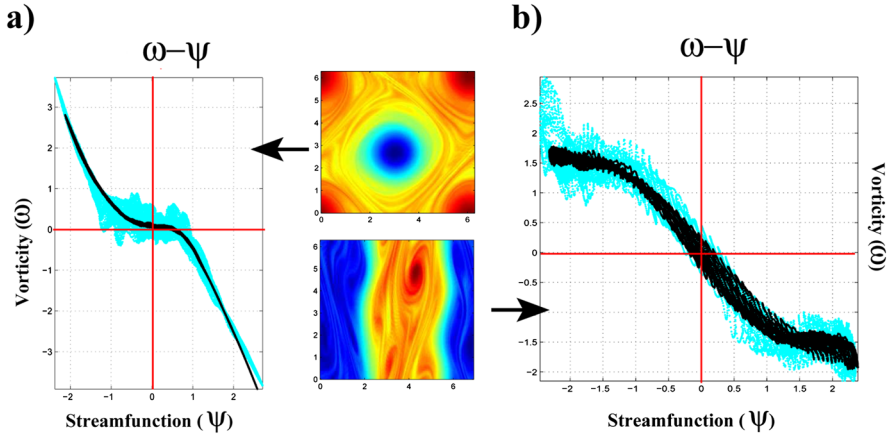

FIG. 3 (color online). $\omega - \psi$ scatterplots (light shade). In black, the same after time averaging (averaging windows $1 \ll \tau \ll 1/\nu$, the drift due to translational invariance has been removed) (a) dipole case with $\delta = 1.03$ (b) unidirectional case $\delta = 1.10$.

firmed both for $\alpha = 0$ and $\alpha \neq 0$, and for different ν values and forcing spectra. The functional dependence between ω and ψ behaves like sinh in the dipole case [Fig. 3(a)] and tanh in the unidirectional case [Fig. 3(b)]. It confirms that the solutions remain close to steady Euler ones.

A very natural order parameter is $|z_1|$, where $z_1 = \frac{1}{(2\pi)^2}\langle\omega(x, y)\exp(iy)\rangle_{\mathcal{D}}$. Indeed, for the unidirectional flows $\omega = \alpha e_1$, $|z_1| = 0$, whereas for a dipoles $\omega = \alpha(e_1 + e_2)$, $|z_1| = \alpha$. Figure 1 shows $|z_1|$ time series for $\delta = 1.02$ and $\delta = 1.04$. The remarkable observation is the bimodal behavior in this transition range. The switches from $|z_1|$ values close to zero to values of order of 0.6 correspond to genuine transitions between unidirectional and dipole flows. The PDF of the complex variable z_1 (Fig. 1) exhibits a circle corresponding to the dipole state (a slow dipole random translation corresponds to a phase drift for z_1, explaining the circular symmetry). The zonal state corresponds to the central peak. As δ increases, one observes less dipole occurrences. For larger (resp. smaller) values of δ, only unidirectional (dipole) flows exist. The transition is also visible for other physical variables: $\Omega_4 = \langle|\omega|^4\rangle_{\mathcal{D}}$ switches between a state with weak variance and low mean value (unidirectional) to an intermittent state with large variance and larger mean value (dipole). Topology changes are very slow dynamical processes: for the model (4), an average transition time is of order $1/\nu$. For instance, Fig. 1 corresponds to 3×10^4 *coherent structure* turnover times. For this reason, due to numerical limitations, it has not been yet possible to obtain convincing statistics for the switches.

In the spirit of [16], we might look for low-dimensional analogies. PDF dependence on the control parameter bears striking similarities with the stochastic differential equation

$$dx = x(\mu + x^2 - x^4)dt + \sigma dW. \tag{9}$$

The deterministic part of (9) is the normal form for a generalized subcritical pitchfork bifurcation. For $\mu < -1/4$, one has a single stable fixed point $x^\star = 0$. For $\mu > 0$, there are three fixed points, one unstable $x_0 = 0$ and two stable $x_{1,2} = \pm[1 + (1 + 4\mu)^{1/2}]^{1/2}$. For $\mu \in [-1/4, 0]$, three stable fixed points coexist (x_0 and $x_{1,2}$) and two unstable ones $x_{3,4} = \pm[1 - (1 + 4\mu)^{1/2}]^{1/2}$. With additive noise ($\sigma \neq 0$), when $\mu < -1/4$, the $|x|$ PDF has a single peak centered at $x = 0$. In the interval corresponding to $\mu \in [-1/4, 0]$, an additional peak appears related to $|x_{1,2}|$. Finally, there is a transition for μ larger than 0 and only one peak corresponding to $|x_1|$ remains.

Using the variational problem (6), we have described a huge ensemble of stable steady states of Euler equations, parameterized by s (or f). We have shown that the detailed shape of s was unimportant, and that only the parameter a_4 has a significant role. Numerical simulations show that, as may have been expected, major changes in the steady state topology, like bifurcations, also occur in the out-of-equilibrium SNS equation context even if there is no known theory that predicts s in such a case. From a theoretical point of view, the main issue, beyond the scope of this Letter, is to explain which of the Euler steady states is actually selected by the turbulent SNS equation (to predict s) and to predict the relative frequency of such states.

Following the same approach, bifurcation diagrams can be computed for any Euler-like model (QG or SW). For geophysical flows, the expected type of topology changes will be strongly affected by the beta effect, topography, stratification, and the domain boundary. In cases where a bifurcation line exists, we also expect similar random flow topology changes, with weak forces and dissipation. We expect this approach to explain the bifurcations observed in [3,6]. However, the range of validity of the approach needs to be assessed more precisely using numerical simulations. Rotating tanks experiments could then be designed in order to observe similar phenomena.

This work was supported by the ANR program STATFLOW (ANR-06-JCJC-0037-01).

*Freddy.Bouchet@inln.cnrs.fr

[1] M. Berhanu, R. Monchaux, S. Fauve, N. Mordant, F. Petrelis, A. Chiffaudel, F. Daviaud, B. Dubrulle, L. Marie, and F. Ravelet *et al.*, Europhys. Lett. 77, 59001 (2007).
[2] F. Ravelet, L. Marié, A. Chiffaudel, and F. Daviaud, Phys. Rev. Lett. **93**, 164501 (2004).
[3] E. R. Weeks, Y. Tian, J. S. Urbach, K. Ide, H. L. Swinney, and M. Ghil, Science **278**, 1598 (1997).
[4] J. Sommeria, J. Fluid Mech. **170**, 139 (1986).
[5] S. R. Maassen, H. J. H. Clercx, and G. J. F. van Heijst, J. Fluid Mech. **495**, 19 (2003).
[6] M. J. Schmeits and H. A. Dijkstraa, J. Phys. Oceanogr. **31**, 3435 (2001).
[7] R. H. Kraichnan, Phys. Fluids **10**, 1417 (1967).
[8] G. L. Eyink and K. R. Sreenivasan, Rev. Mod. Phys. **78**, 87 (2006).
[9] M. Chertkov, C. Connaughton, I. Kolokolov, and V. Lebedev, Phys. Rev. Lett. **99**, 084501 (2007).
[10] S. B. Kuksin, J. Stat. Phys. **115**, 469 (2004).
[11] D. Marteau, O. Cardoso, and P. Tabeling, Phys. Rev. E **51**, 5124 (1995).
[12] K. Schneider and M. Farge, Physica D (Amsterdam) **237D**, 2228 (2008).
[13] (a) V. I. Arnold, Dokl. Akad. Nauk SSSR **162**, 975 (1965); (b) V. I. Arnold. On one *a priori* estimate in the theory of the hydrodynamical stability. Izv. VUZov, Ser. Mat. **5**, 3 (1966).
[14] F. Bouchet, Physica D (Amsterdam) **237D**, 1976 (2008).
[15] Z. Yin, D. C. Montgomery, and H. J. H. Clercx, Phys. Fluids **15**, 1937 (2003).
[16] R. Benzi, Phys. Rev. Lett. **95**, 024502 (2005).